JOURNAL OF MATERIALS SCIENCE 5 (1970) 9–23

Compatibility Studies of Carbon Fibres with Nickel and Cobalt

P. W. JACKSON, J. R. MARJORAM
Rolls-Royce Limited, Advanced Research Laboratory, Old Hall, Littleover, Derby, UK

Techniques have been evolved to study the compatibility of single carbon fibres coated with nickel or cobalt, and the results have been shown to be applicable to bulk composites. Carbon fibres undergo structural recrystallisation in contact with the nickel or cobalt matrix by a dissolution/diffusion/reprecipitation mechanism. The effective activation energy for this recrystallisation process approximates that for carbon diffusion in nickel or cobalt.

1. Introduction

Carbon fibres of high strength and stiffness have recently been developed [1, 2] and are now available in production quantities. By analogy with bulk graphite, the mechanical properties of these fibres should still be attractive at high temperatures. However, in order to utilise these properties, a suitable matrix material must be found which neither reacts with, nor causes degradation of, the fibres. Unfortunately, carbon forms stable carbides with most refractory metals such as chromium, titanium, niobium and molybdenum, and is soluble to some extent in the solid state in most other high melting point metals, such as nickel, cobalt and platinum.

The solid solubility of carbon in nickel and cobalt increases with temperature as shown in fig. 1 [3]. Johnson [4] found that removal of the surface by argon ion-bombardment did not decrease the strength of carbon fibres. On this basis, dissolution of the carbon fibre surface by nickel or cobalt during heat-treatment at elevated temperatures would be expected to leave the fibre properties substantially unimpaired. Early results from heat-treatment of nickel-coated fibres at 1100° C [5] suggested that this was not the case; structural recrystallisation of the fibres occurred in the presence of nickel or cobalt, accompanied by a marked fall in the fibre strength. Further studies were therefore performed and are reported in the present paper.

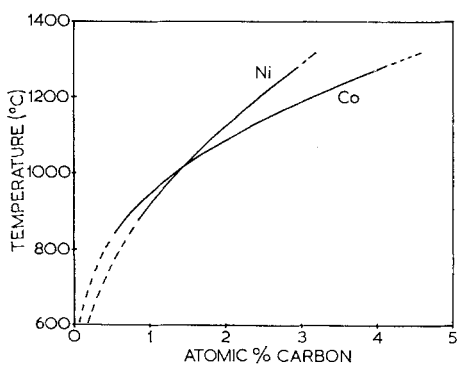

Figure 1 Solid solubility of carbon in nickel and cobalt.

© *1970 Chapman and Hall Ltd.*

2. Experimental

2.1. Fibre Characteristics

Two types of carbon fibres were used in the present investigations: (a) carbonised fibres (subsequently referred to as C fibres), prepared by controlled pyrolysis of polymer fibres at temperatures up to ~ 1000° C; (b) graphitised fibres (subsequently referred to as G fibres), prepared by pyrolysis up to ~ 2700° C.

Both types of fibre are polycrystalline, having graphite basal planes preferentially oriented along the fibre axis, but turbostratically misplaced relative to each other [6]. The [002] directions in adjacent regions are randomly arranged, approximately within a plane normal to the fibre axis, the degree of alignment being higher in graphitised fibres. The effective crystallite size and crystallite perfection are improved by the higher processing temperature. C fibres also contain considerable quantities of nitrogen

TABLE I Properties of carbon fibres

Type of fibre	Fibre breaking stress, lb/in.^{2} × 10^3	Fibre modulus, lb/in.^{2} × 10^6	Mean area/ fibre, in.^{2} × 10^{-8}	Crystallite size, L_c Å	Interlayer spacing, $d_{(0\,0\,2)}$Å
Carbonised	176 ± 28%	24.5 ± 5%	9.24 ± 7%	10.5	3.61
Graphitised (Batch A)	269 ± 23%	55.5 ± 10%	13.2 ± 14%	—	—
Graphitised (Batch B)	254 ± 24%	60.1 ± 5%	6.39 ± 14%	73	3.42

1 lb/in.^{2} = 0.0703 kg/cm^2 = 6894.76 N/m^2.

and hydrogen, whereas the G fibres are virtually pure carbon. The characteristics and properties of the fibres are detailed in table I. The initial strength, modulus and mean fibre cross-sectional area values were obtained from measurements of 12 single fibre samples from each batch.

2.2. Fibre Strength Tests

The strength of the fibres was evaluated in the present series of experiments by using a microcomposite method suggested by Mallinder [7]. This technique uses about 15 fibres rather than a single fibre in order to facilitate handling and to attempt to reduce the scatter of the results. Thus approximately 15 carbon fibres at a time were mounted on a frame using a conductive thermosetting silver preparation to ensure adequate electrical contact. The fibres were then electroplated with a coating of nickel or cobalt equivalent to ~ 20 vol % metal, using the electroplating baths detailed in table II. This coating was considered to be thin enough for its cross-sectional area to be ignored in comparison with the strong fibres. The metal-coated and uncoated C and G fibres were then heat-treated as bundles of about 15 fibres in vacuum at temperatures up to 1100° C for times from 1 h to 1 week.

After heat-treatment the fibre bundles were converted to microcomposites by applying a few drops of Araldite MY 753/HY 951 resin to each bundle and allowing the excess to drain off vertically during curing of the resin. These microcomposites were fractured in tension and the broken pieces were mounted, sectioned and polished for examination. The strength of the fibres was estimated from the breaking load of the microcomposite, the number of fibres in each microcomposite and the mean fibre cross-sectional area for the relevant batch of fibre (see table I). No "bundle strength" corrections were applied. Previous experience with various metal-coated fibres [8] suggested that any contribution to the strength from the metal coating or the resin was negligible.

2.3. Microscopy

Samples of coated and uncoated C and G fibres were examined by optical microscopy both before and after heat-treatment. Additionally, some use was made of the unique capabilities of the Stereoscan scanning electron microscope to look at surfaces and fracture faces of the fibres. Fibres were also examined after etching with a 50% nitric acid, 25% acetic acid, 25% water solution to remove the metal coating and, in an attempt to reveal structure within the fibres themselves, after argon ion-bombardment on a few selected samples.

2.4. X-Ray Diffraction Studies

The fibre bundles were lightly ground to a powder in a small agate mortar, mounted in Lindemann glass tubes of about 0.3 mm diameter and exposed to nickel-filtered copper Kα radiation in a 114.6 mm diameter Philips Debye-Scherrer powder camera.

The diffraction patterns from early specimens of nickel and cobalt-coated fibres before and after heat-treatment at 1100° C showed no signs of nickel (or cobalt) carbide formation [5] so

TABLE II Nickel and cobalt electroplating solutions

Nickel	Cobalt
"Nispeed"	
Nickel sulphamate, $Ni(SO_3NH_2)_2.4H_2O$ 600 g/l	Cobalt sulphate, $CoSO_4.7H_2O$ 400 g/l
Nickel chloride, $NiCl_2.6H_2O$ 10 g/l	Cobalt chloride, $CoCl_2.6H_2O$ 40 g/l
Boric acid, H_3BO_3 40 g/l	Boric acid, H_3BO_3 40 g/l
pH ~ 4, temperature ~ 60° C	pH ~ 4, temperature ~ 35° C

subsequently the metal coating was removed by etching before exposure.

The crystallograms allowed changes in the structure during recrystallisation to be followed and the graphite (002) reflection to be measured. From a microdensitometer trace across this arc an effective crystallite size or perfection parameter, L_c, was determined by conventional line broadening procedure and a mean interlayer spacing $d_{(0\,0\,2)}$ estimated. In this study no attempt has been made to apply the usual corrections to the profiles since only comparative values, reflecting the state of order within the fibre, were required.

2.5. C, H, N Analysis

The C fibres still contained considerable quantities of elements other than carbon and it was of interest to determine the effects of heat-treatment on these elements, particularly in the presence of a nickel coating. Samples of the uncoated C fibre were analysed as-received and after heat-treatment for 1 day at 800 and 1100° C respectively. Nickel-coated C fibres were also heat-treated for a day at 800 and 1100° C respectively. Analyses were performed using a combustion/gas chromatography technique [9].

3. Results

3.1. Fibre Strength Tests

Heat-treatment for a day at temperatures up to 1100° C produced no significant changes in the strength of uncoated C and G fibres, as shown in figs. 2 and 3 respectively. The effect of a nickel coating on the C and G fibres is shown in figs. 4 and 5 respectively, whilst the effect of a cobalt coating on G fibres is shown in fig. 6. A marked fall in strength was observed after 1 day above

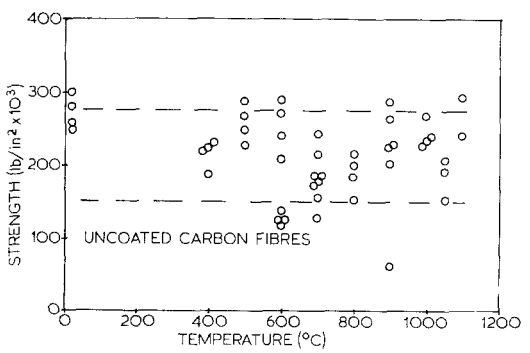

Figure 2 Strength of uncoated C fibres after heat-treatment for 1 day.

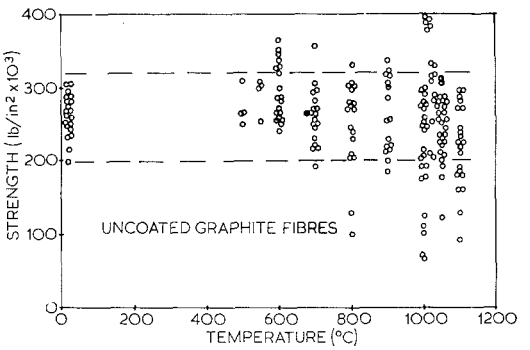

Figure 3 Strength of uncoated G fibres after heat-treatment for 1 day.

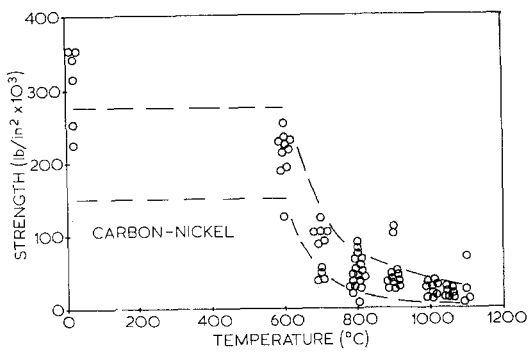

Figure 4 Strength of nickel-coated C fibres after heat-treatment for 1 day.

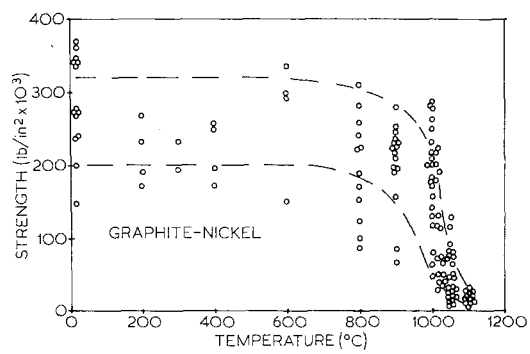

Figure 5 Strength of nickel-coated G fibres after heat-treatment for 1 day.

~ 700° C (C–Ni), ~ 1000° C (G–Ni), and ~ 1000° C (G–Co). The additional effect of time at temperature is shown in the temperature/time diagrams of figs. 7, 8 and 9. The full data are given in table III.

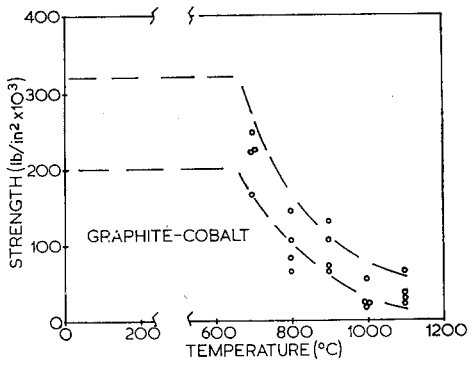

Figure 6 Strength of cobalt-coated G fibres after heat-treatment for 1 day.

The scatter shown in these microcomposite strength results is disappointingly high in many cases. Results from microcomposites made with undegraded fibres generally show more consistency than is found in single fibre tests. However, microcomposite test results in the intermediate strength range, in particular, tended to display more scatter than would normally be expected from even single fibres. This discrepancy is probably a consequence of the sensitivity of the fibres to the various experimental conditions employed.

Some anomalies occurred in room temperature test results from C fibres; single fibre

TABLE III Fibre strength and crystallite size data from heat-treatment of nickel and cobalt-coated fibres

(*a*) C Fibres/Nickel

Heat-treatment temp, ° C	time, h	Crystallite size, L_c Å	Interlayer spacing, $d_{(0\,0\,2)}$ Å	Fibre breaking stress, lb/in.² × 10^3
—	—	10.8	3.557	226, 253, 316, 343, 354, 354
600	24	10.7	3.623	125, 188, 190, 213, 217, 224, 231, 231, 233, 253
600	168	11	3.562	94, 101, 137, 146, 146, 150, 193
650	96	12	3.566	222, 228, 240, 264
700	1	10.4	3.587	193, 206, 213, 246
700	4	10.2	3.603	132, 155, 175, 222
700	15	10	3.616	121, 128, 146, 157
700	16	10.5	3.609	76, 87, 105
700	24	12.8	3.552	38, 38, 47, 54, 87, 92, 107, 107, 107, 123
700	48	71	3.383	38, 49, 105, 125
750	7.5	10	3.594	159, 163, 193, 193
750	16	—	—	36, 56, 60, 101
800	1	13	3.538	166, 177, 179, 206
800	5	30	3.403	36, 72, 76, 81
800	24	52 60	3.410 3.402	4, 20, 25, 34, 36, 36, 40, 43, 43, 45, 47, 47, 47, 54, 58, 63, 69, 74, 83, 90
850	1	58	3.402	27, 49, 60, 81
900	1	62	3.389	22, 38, 45, 157
900	24	63	3.399	25, 29, 31, 31, 34, 36, 38, 43, 47, 51, 101, 112
1000	24	370	3.356	9, 11, 16, 27, 31, 31, 34, 36
1050	24	—	—	11, 13, 16, 18, 20, 27, 29
1100	24	1000	3.361	4, 11, 25, 69

(*b*) G Fibres (Batch A)/Nickel

Heat-treatment temp, ° C	time, h	Fibre breaking stress, lb/in.² × 10^3
—	—	148, 202, 237, 240, 273, 273, 273, 278, 336, 340, 340, 347, 361, 369
200	24	170, 190, 233, 269
300	24	195, 233
400	24	172, 195, 249, 257
600	44	150, 291, 298, 336
800	24	87, 101, 123, 155, 170, 188, 220, 224, 242, 258, 282, 309
900	24	67, 81, 157, 188, 193, 197, 208, 217, 222, 222, 229, 229, 235, 247, 251, 278
1000	24	47, 63, 81, 128, 141, 168, 177, 181, 199, 199, 217, 217, 249, 262, 276, 278, 287
1010	24	29, 45, 116, 116
1020	24	45, 51, 72, 74, 114, 128, 190, 222
1030	24	36, 38, 49, 65
1050	24	2, 9, 11, 13, 13, 20, 22, 34, 38, 47, 52, 58, 63, 72, 112, 141, 170, 177, 183
1060	24	18, 31, 31, 45
1100	24	9, 11, 18, 18, 18, 20, 22, 27, 27, 27, 29, 29, 31

TABLE III continued

(*c*) G Fibres (Batch B)/Nickel

Heat-treatment temp, ° C	time, h	Crystallite size, L_c Å	Interlayer spacing, $d_{(0\,0\,2)}$ Å	Fibre breaking stress, lb/in.^{2} × 10^3
800	168	67	3.431	90, 96, 107
850	168	72	3.431	45, 69, 96, 99, 123, 148
900	50	—	—	141, 229, 231, 235
900	96	72	3.429	20, 52, 92, 116
900	168	—	—	69, 78, 81, 83, 87, 96, 108, 114, 125, 217
950	96	68	3.428	29, 94, 114, 121
1000	1	68	3.421	222, 224, 258, 260
1000	5	70	3.423	235, 240, 264, 298
1000	24	71	3.424	157, 177, 199, 208, 231
1000	36	65 and 200	3.399 and 3.364	83, 130, 177, 193
1000	48	>1000	3.358	25, 34, 36, 60
1000	100	>1000	—	4, 4, 4, 13
1050	5	66	3.418	155, 206, 267, 381
1050	13	500	3.356	56, 141, 161, 161
1050	24	—	—	47, 67, 70, 74, 76, 92, 116, 130
1100	1	72	3.423	130, 172, 188, 202
1100	5	650	3.362	22, 29, 85, 94
1100	24	>1000	3.356	

(*d*) G Fibres (Batch B)/Cobalt

Heat-treatment temp, ° C	time, h	Crystallite size, L_c Å	Interlayer spacing, $d_{(0\,0\,2)}$ Å	Fibre breaking stress, lb/in.^{2} × 10^3
700	24	80	3.426	166, 222, 224, 249
800	24	75	3.432	65, 83, 107, 145
900	24	71	3.431	65, 69, 107, 132
900	62	70	3.426	45, 63, 76, 78
950	50	67 and 200	(3.402)	
1000	16	57 and 200	3.421 and 3.367	45, 69, 81, 85
1000	24	1000	3.362	20, 22, 22, 56
1100	1	1000	3.361	52, 60, 65, 81
1100	24	1000	3.361	22, 31, 36, 65

1 lb/in.^{2} = 0.0703 kg/cm^2 = 6894.76 N/m^2.

strengths (176000 lb/in.^{2} ± 28 %) were not in good agreement with uncoated nor with nickel-coated C fibre microcomposite strengths (means 273000 and 307000 lb/in.^{2} respectively). The two sets of results fall at either end of the overall C fibre microcomposite scatter band (fig. 2). This difference is puzzling since previous single fibre and microcomposite experience with a variety of carbon fibre batches and metal coatings [7, 8] has suggested good agreement. However, conclusions may still be drawn from the current C fibre microcomposite results on a *comparative* basis, even if their *absolute* values are open to some doubt.

3.2. Microscopy

Nickel or cobalt-coated fibres heat-treated at temperatures which did not cause degradation showed no noticeable changes in fibre structure when polished cross-sections were examined using the optical microscope. Stereoscan photographs of the surface of nickel-coated G fibres after heat-treatment for one day at 800° C (i.e. no strength degradation) and subsequent removal of nickel showed some pitting of the fibre surface due to dissolution of surface carbon atoms in the nickel (fig. 10). The general topography of the surface, however, appeared unchanged. At higher temperatures (associated

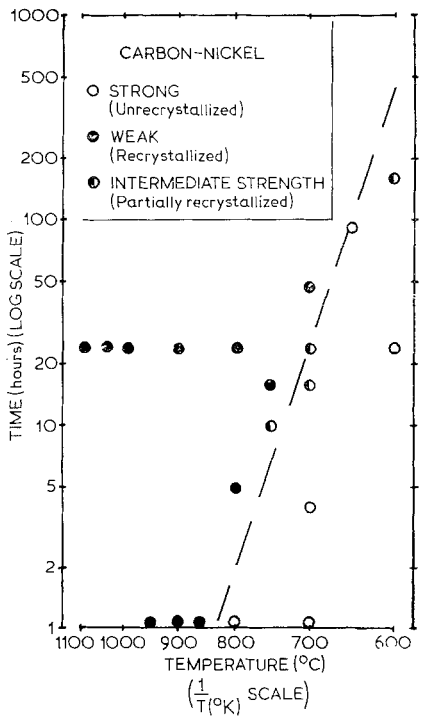

Figure 7 Temperature/time stability of nickel-coated C fibres.

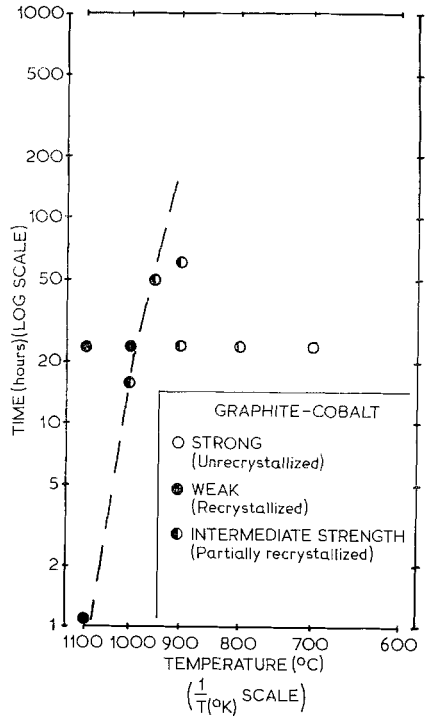

Figure 9 Temperature/time stability of cobalt-coated G fibres.

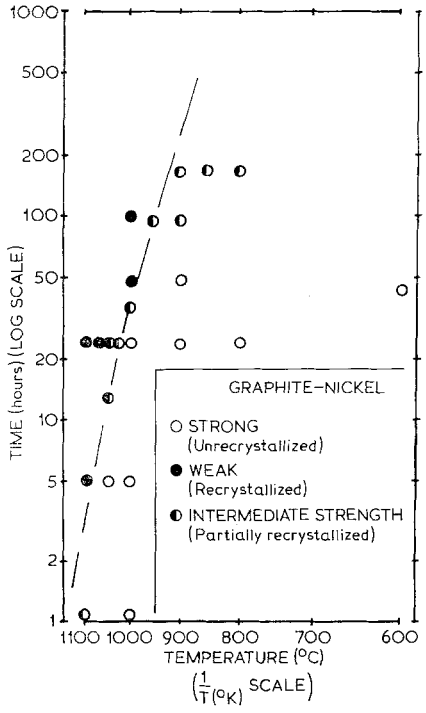

Figure 8 Temperature/time stability of nickel-coated G fibres.

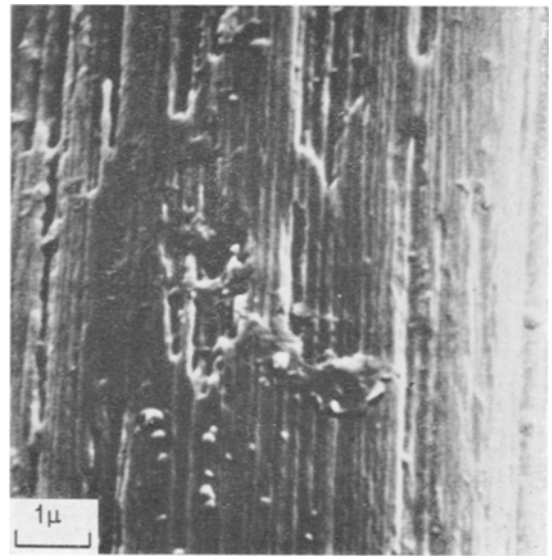

Figure 10 Pitting of nickel-coated G fibre from heat-treatment for 1 day at 800° C.

with severe loss of strength), the longitudinal markings present on the original G fibres tended to disappear and the fibre surface became smooth and featureless, as shown in fig. 11.

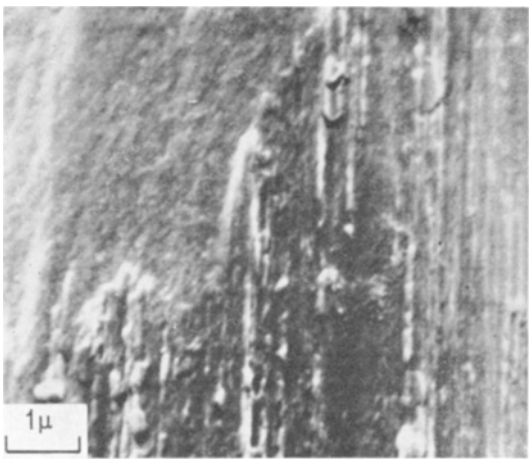

Figure 11 Smoothing of nickel-coated G fibre surface from heat-treatment for 1 day at 1050° C.

A more detailed examination was conducted on some nickel-coated G fibres after heat-treatment for 5 days at 1100° C. A Stereoscan picture of heat-treated fibre surface and fracture face is shown in fig. 12b. The whole of the ~ 20 vol % nickel coating does not appear to be present on the fibre surface, even allowing for the nickel visible as small spheres; also the appearance of the fracture face is totally different to that usually observed with G fibres (fig. 12a). Optical examination of polished cross-sections of the heat-treated fibres confirmed the presence of nickel within the fibres, as illustrated in fig. 13, which also shows fibres joined together, i.e. graphite to graphite. Later Stereoscan observations on specimens which were heavily etched by argon ion-bombardment confirmed this view of continuity of structure across a pair of fibres, as shown in fig. 14. (Argon ion-bombardment etching of normal G fibre will eventually remove the original longitudinal markings, smoothing the fibre surface without revealing any details of the fibre structure; thus the relatively coarse structure found here is *not* typical of normal G fibre.)

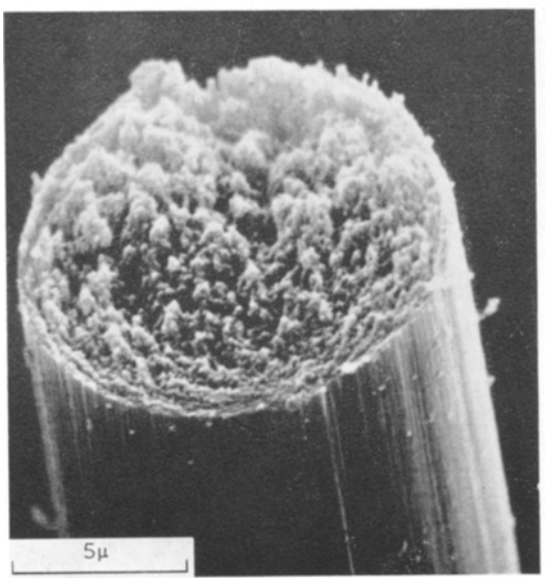

(a)

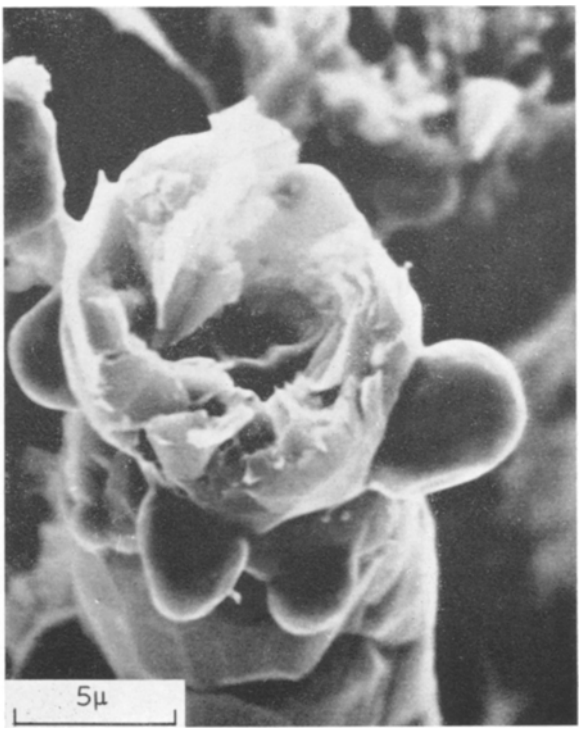

(b)

Figure 12 Fracture faces of (a) original uncoated G fibre, (b) nickel-coated G fibre after heat-treatment for 5 days at 1100° C.

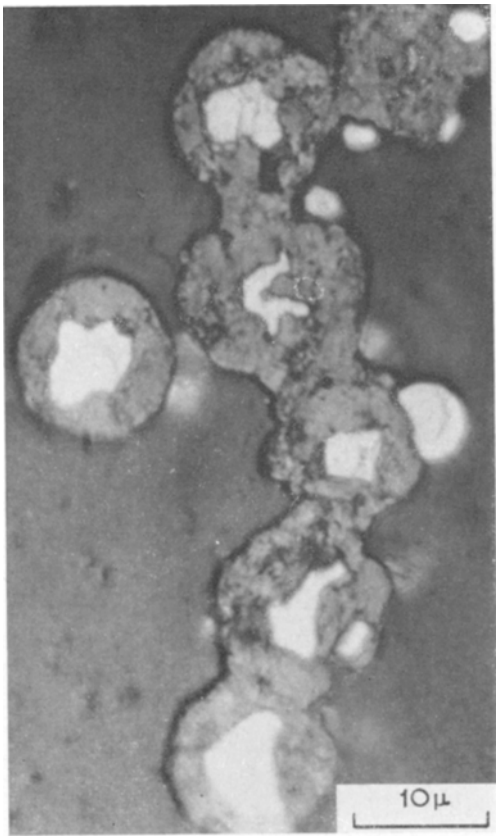

Figure 13 Cross-sections of nickel-coated G fibres after heat-treatment for 5 days at 1100° C.

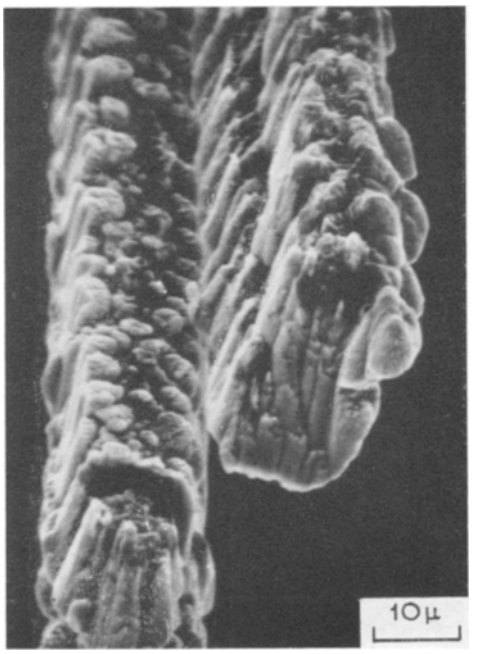

Figure 14 Nickel-coated G fibres heat-treated for 5 days at 1100° C, after argon ion-bombardment etching.

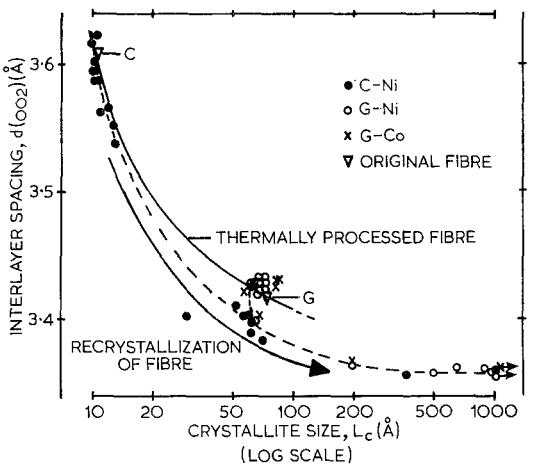

Figure 15 Relationship between interlayer spacing and effective crystallite size for thermally processed and recrystallised carbon fibres.

3.3. X-Ray Diffraction Studies

X-ray crystallography has proved particularly rewarding in characterising the changes which take place within C and G fibres on heat-treatment in a nickel or cobalt environment.

Measurements of crystallite size and inter-layer spacing for carbon fibres, processed in an inert atmosphere *without* a metal present at temperatures up to ~ 3000° C, have established a relationship between these parameters which represents the growth of order in the turbostratic crystallite structure of the fibres. This relationship for thermally processed fibres is given in fig. 15 (solid line) together with the results from the present metal-coated samples (dashed lines).

The first indication of structural change in the G fibres is a slight decrease in the measured L_c value without the expected corresponding change in interlayer spacing. This apparently anomalous effect may be explained by supposing that the initial recrystallisation mechanism involves the movement of basal dislocations at crystallite boundaries so as to produce a proportion of smaller crystallites and a few larger ones. These small crystallites would unduly weight the L_c value obtained from line-broadening and result in a fractionally smaller measured value. This

initial reduction in L_c is also suggested in the results from C fibres, but because of the very much more disordered structure of these fibres (as indicated by the L_c and $d_{(0\,0\,2)}$ values themselves), it is much more difficult to establish.

With further heat-treatment of both types of fibre the crystallite size increases and the mean interlayer spacing decreases, indicating that an improvement in crystalline order is taking place. In some cases it has been apparent that initially only part of the fibres has started to recrystallise because the crystallograms have shown two populations of sizes, one corresponding approximately to that of the initial fibre and one somewhat larger. Fig. 16 shows a microdensitometer trace of the profile of the graphite (002) diffraction arc of such a specimen and, for comparison, traces from original and fully recrystallised G fibres.

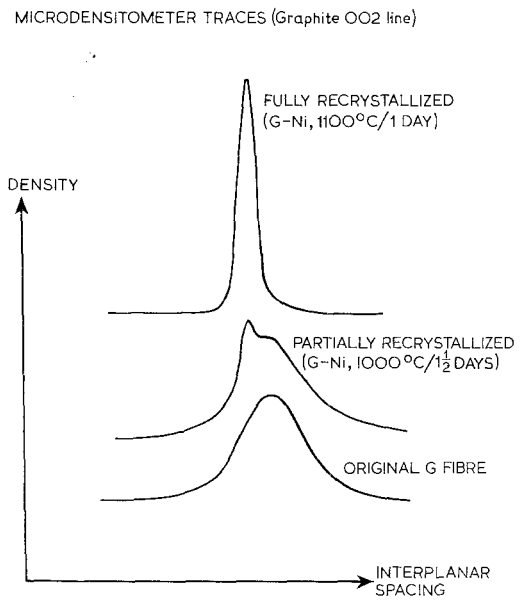

Figure 16 Microdensitometer traces of the (002) line for various fibres.

Finally the crystallites become so large that they can often be distinguished in the optical microscope. Three-dimensional diffraction lines, such as (101) and (112), appear during this growth process and the diffraction pattern becomes identical with that of natural graphite. These features clearly show that true recrystallisation is occurring and that the crystallites are not aggregates of the turbostratic crystallites present in the original fibre. Fig. 17 shows a diffraction pattern of such a recrystallised fibre and that of the original G fibre for comparison.

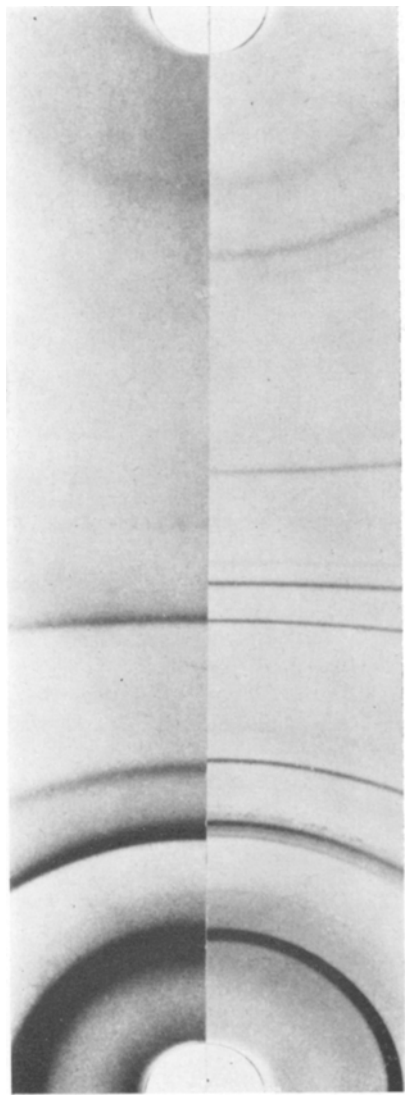

Figure 17 X-ray powder diffraction patterns, (a) original G fibre, (b) recrystallised G fibre, after heat-treatment for 1 day at 1100° C.

The relationship between crystallite size and interlayer spacing which represents the path of recrystallisation for these metal-coated fibres, as shown in fig. 15, is seen to be very different from that of the thermally processed fibre. This difference is confirmation that the mechanism of

structural rearrangement in the two cases is distinct and underlines that true crystallisation is occurring in the presence of nickel or cobalt.

3.4. C, H, N Analysis

The results are shown in full in table IV. Heat-treatment of uncoated C fibres for a day at 800° C caused a slight increase in crystallite size, accompanied by a marked decrease in hydrogen content and a slight decrease in nitrogen content. The addition of a nickel coating resulted in little further change in hydrogen or nitrogen content, although a substantial increase in crystallite size occurred.

Heat-treatment of uncoated C fibres for a day at 1100° C resulted in a somewhat larger increase in crystallite size than at 800° C, but no further change in the hydrogen content and a more substantial drop in the nitrogen content. The addition of a nickel coating resulted in complete recrystallisation of the fibre and the complete elimination of the hydrogen and all but a trace of the nitrogen.

4. Discussion

4.1. Comparisons with Other "Activation" Processes

There have been several reports in the literature on the effects of various metallic elements on the graphitisation of carbons. Yokokawa *et al* [10], examined several metallic compounds and found that those containing copper, nickel, cobalt, manganese and aluminium produced noticeable effects within an hour at 1500° C, a temperature which exceeds the melting point of all these metals. From their data, the order of decreasing effectiveness appeared to be cobalt, nickel, copper, aluminium, manganese. Schwartz and Bokros [11] reported catalytic graphitisation of carbon by titanium, although in this case a temperature of over 2000° C was required before significant effects were observed.

At somewhat lower temperatures, Bokros [12] reported transport of carbon through nickel exposed to graphite isothermally for prolonged periods at temperatures in excess of 900° C, resulting in the growth of particles of graphite within the nickel. This effect was enhanced considerably during thermal cycling between 550 and 1000° C, by a dissolution/diffusion/reprecipitation mechanism. These results suggest the possibility of transport of carbon atoms through nickel to aid recrystallisation of fibres to a more fully graphitic state.

There are many kinds of examples of the effects of additives in enhancing transport mechanisms. A small quantity of a liquid phase can stimulate sintering, for instance by local improvement in diffusion rates [13]. Whisker growth has in many instances been shown to occur, assisted by the enhanced diffusion rates provided by the liquid phase present at the growing tip during the VLS growth mechanism [14]. Growth of diamonds from graphite in the presence of molten nickel under pressure has been found to occur via transport of the carbon atoms through the nickel [15, 16]. However, enhanced diffusion rates can also be obtained with additions that remain completely in the solid state, perhaps the best-documented example being the activated sintering of tungsten [17, 18].

It is interesting to compare in some detail both the present results and those of Bokros [12] with observations that have been made on activated

TABLE IV C, H, N analyses of C fibres

Treatment	Crystallite size, L_c Å	C wt %	H wt %	N wt %	* Remainder wt %
As-received C fibre	10.5	86.96	0.50	10.67	1.87
		(88.61)	(0.51)	(10.88)	
Uncoated C fibre	11.9	87.30	0.15	9.92	2.63
H/t 800° C, 1 day		(89.66)	(0.15)	(10.19)	
Nickel-coated C fibre	52,	84.98	0.16	9.44	5.42
H/t 800° C, 1 day	60	(89.85)	(0.17)	(9.98)	
Uncoated C fibre	14	92.97	0.17	3.56	3.3
H/t 1100° C, 1 day		(96.14)	(0.18)	(3.68)	
Nickel-coated C fibre	>1000	98.51	Nil	0.59	0.9
H/t 1100° C, 1 day		(99.4)	(Nil)	(0.6)	

*This remainder figure may include adsorbed or combined oxygen and unremoved nickel. The C, H, N values in brackets were obtained by scaling up to give 100% C, H, N, which is probably a more consistent standard for comparison.

sintering of tungsten powders and recrystallisation of tungsten fibres. Toth and Lockington [18] and Brophy *et al* [17], have shown that very small amounts of nickel or other Group VIII elements, present as a thin coating on tungsten powder particles or infiltrated into green tungsten powder compacts, can enable near theoretical density to be achieved on sintering at a temperature of only 1100° C for up to 16 h. (Without additive, tungsten requires a sintering temperature of 3000° C.) Vacek [19] has reported rapid densification in tungsten containing very small amounts of iron, cobalt and nickel at temperatures from 1000 to 1300° C. Petrasek and Weeton [20] examined the effects of various binary copper alloy matrices during infiltration for 1 h at 1200° C on tungsten wires used for reinforcement. The effect on the tungsten wire varied with the alloying element (copper itself having no effect on tungsten). With additions of nickel, cobalt or aluminium, a diffusion-penetration reaction occurred, accompanied by recrystallisation of the grains at the periphery of the tungsten fibre. Recrystallisation of this type was not observed when the copper matrix was alloyed with chromium, niobium, titanium or zirconium.

There are some interesting similarities between the nickel-carbon system and the nickel-tungsten system (fig. 18):

(i) both carbon and tungsten have high melting points;

(ii) both systems contain a simple eutectic;

(iii) both carbon and tungsten show considerable solubility in nickel in the solid state (although carbon is interstitial and tungsten substitutional);

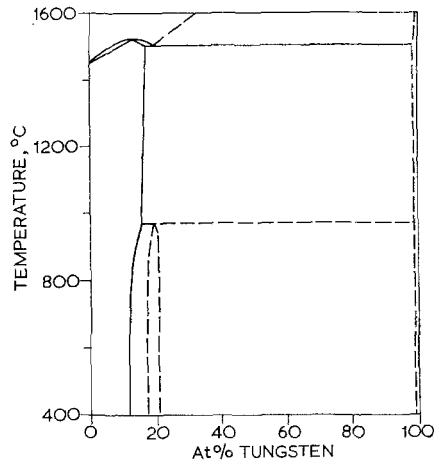

Figure 18 Nickel-tungsten equilibrium diagram [22].

(iv) the solid solubility of nickel is low in both graphite and tungsten;

(v) the surface and volume diffusion rates of tungsten in nickel are considerably higher than those of nickel in tungsten [19]; being an interstitial element, the diffusion rate of carbon in nickel would be expected to be considerably more rapid than that of nickel in graphite.

It is also interesting to note that equilibrium diagrams, similar in most of the above charac-

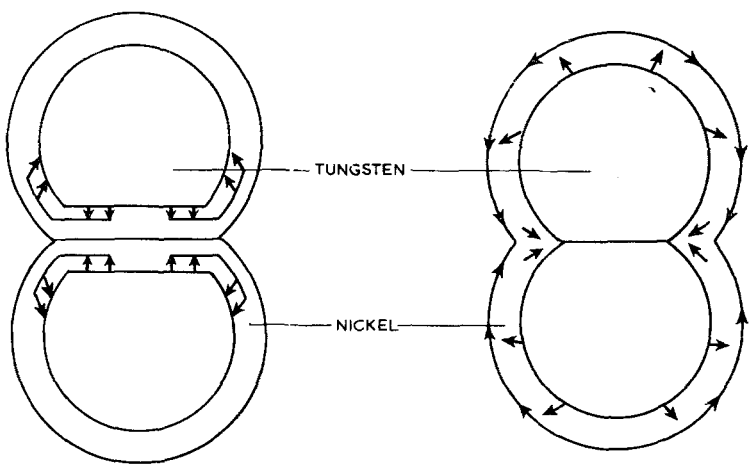

Figure 19 Proposed mechanisms for transport of tungsten atoms via nickel, (a) Brophy *et al* [17], (b) Toth and Lockington [18].

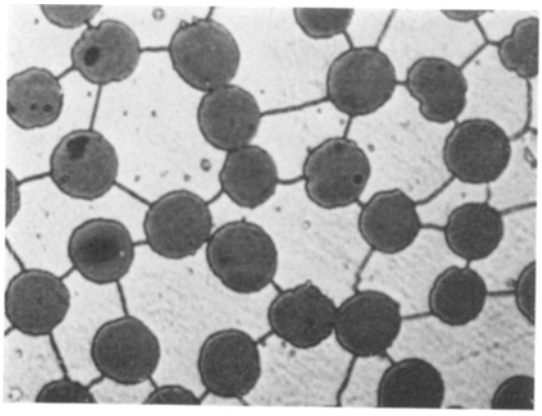

(a)

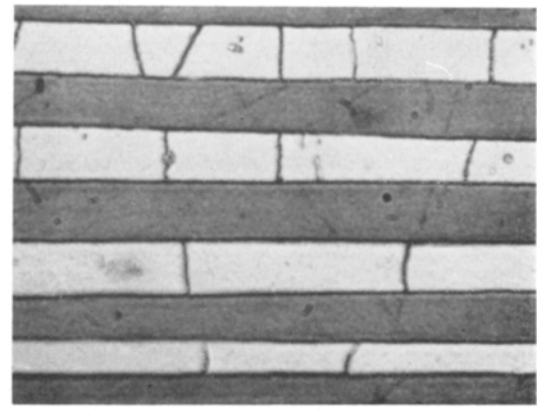

(b)

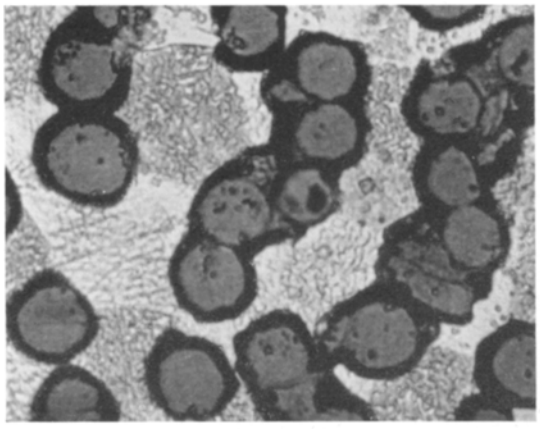

(c)

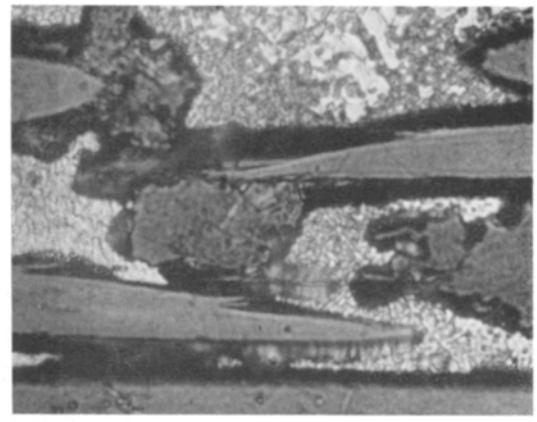

(d)

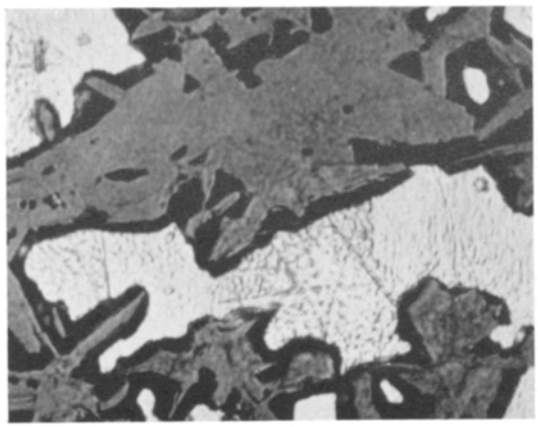

(e)

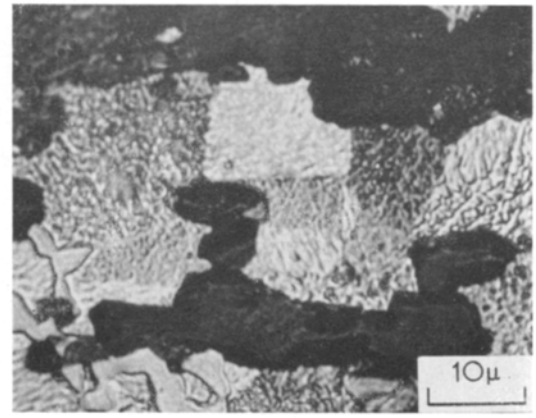

(f)

Figure 20 G fibre/nickel composite: (a), (b) as-hot-pressed, (c), (d) heat-treated for 4 days at 1000° C, (e), (f) heat-treated for 4 days at 1100° C.

teristics, are obtained from systems consisting of tungsten with the metals iron, cobalt, palladium, rhodium, platinum or ruthenium, all of which are capable of enhancing sintering and/or recrystallisation in tungsten. However, considering the metals chromium, niobium, titanium and zirconium where this effect was not observed, it is interesting to note that the equilibrium diagrams for these metals with tungsten are very different from that for nickel with tungsten; chromium and niobium are completely mutually soluble in both the liquid and solid states at high temperatures; both titanium and zirconium show regions of notable solid solubility at both the tungsten-rich and the titanium/zirconium-rich ends of the diagram.

Brophy *et al* [17] have proposed a mechanism for the role of nickel or palladium in the activated sintering of tungsten and more recently some of the details of this have been refined by Toth and Lockington [18]. Their tungsten transport mechanisms are illustrated by the sketches shown in fig. 19 and it is interesting to compare these with the coalesced G fibres illustrated in figs. 13 and 14. The reason for the migration of the nickel towards the centre of the fibres as in fig. 13 is perhaps at first less clear. However, the thin nickel coating has been observed to spheroidise during heat-treatment at high temperatures. The driving force for this process is the reduction in nickel surface energy and it would tend to take place at temperatures where nickel self-diffusion was significant; this would certainly be the case at 1100° C. Once the nickel coating has been converted to small spheres, a further reduction in the nickel surface energy can only be achieved by the coalescence of small spheres to form larger spheres. This can occur by the movement of carbon atoms through the nickel during fibre recrystallisation, causing a net movement of the nickel towards the recrystallised fibre centre.

Support for this view also comes from heat-treatment studies of hot-pressed composites, consisting of ~ 50 vol % of C or G fibres in a nickel matrix. The microstructural changes observed during recrystallisation are illustrated in fig. 20. After pressing (fig. 20a and b), the fibres retain their normal shape and there is no tendency for any stray graphite to intrude. Heat-treatment at 1000° C for 4 days, although showing no substantial change in the mean crystallite size as determined by X-ray measurements, did result in the appearance of some traces of graphite "fingers" in the microstructure (fig. 20c and d). Heat-treatment at 1100° C for 4 days resulted in complete fibre recrystallisation to a fully graphitic state and an interlinked network of large flaky particles of graphite (fig. 20e and f) many of them surrounding small regions of nickel, as previously observed with nickel-coated fibres.

4.2. Kinetic Effects

By representing the data in the log t vs. $1/T$ form of figs. 7, 8 and 9, a line can be drawn which indicates approximately the onset of fibre recrystallisation. The slope of this line can be used to calculate approximately an effective activation energy for the recrystallisation process, viz:

C–Ni ~ 50 kcal/mol
G–Ni ~ 50-80 kcal/mol
G–Co ~ 80 kcal/mol

The nickel values may be compared with the published value for the activation energy for carbon diffusion in nickel of ~ 40 kcal/mol [21]. The present data, although somewhat approximate, are not inconsistent with this figure, although it is probable that other factors are also playing a part as shown by, for instance, the change of slope in the G–Ni system (fig. 8). The activation energy data thus broadly support the view that fibre recrystallisation proceeds by means of carbon diffusion through the nickel. The G–Co value is particularly approximate, because of the very limited number of data points (fig. 9). However, the overall similarity of behaviour to G–Ni suggests that a similar recrystallisation mechanism is operating.

The marked difference in the behaviour of C and G fibres (figs. 7 and 8) is particularly interesting. The activation energy data for the nickel-aided recrystallisation of the two kinds of fibre suggest that the final rate controlling mechanism is probably the same in both cases, i.e. the process of carbon diffusion through the nickel. However, before this can take place, the carbon atoms must be detached from the fibres and enter into solid solution in the nickel. C fibres differ from G fibres in two ways, both of which tend to increase their relative structural instability, thereby facilitating the initial dissolution process:

(a) C fibres have a more disordered structure, as indicated by the smaller effective crystallite size values and greater interlayer spacing values than those found in G fibres;

(b) C fibres contain significant quantities of nitrogen and hydrogen within the structure.

The data from C, H, N analyses (table IV) and the associated crystallite size data, show that considerable recrystallisation of C fibres can take place without significant loss of nitrogen, as shown by the increase in crystallite size to 60 Å (i.e. close to the 70 Å of the original G fibre) after heat-treatment of nickel coated C fibre at 800° C. Conversely, loss of significant amounts of nitrogen does not automatically result in a large increase in crystallite size, as shown by the heat-treatment of uncoated C fibres at 1100° C. The data are consistent with the nitrogen being tolerated in the fibre structure, as part of the "graphite" basal planes, during the early stages of recrystallisation, i.e. whilst the crystallite size is increasing but before there is any real sign of three-dimensional order. However, when a fully ordered graphite state is achieved, e.g. after heat-treatment of nickel-coated C fibres at 1100° C, it appears that nitrogen can no longer be retained in large quantities, since the nitrogen would disrupt the orderly structure.

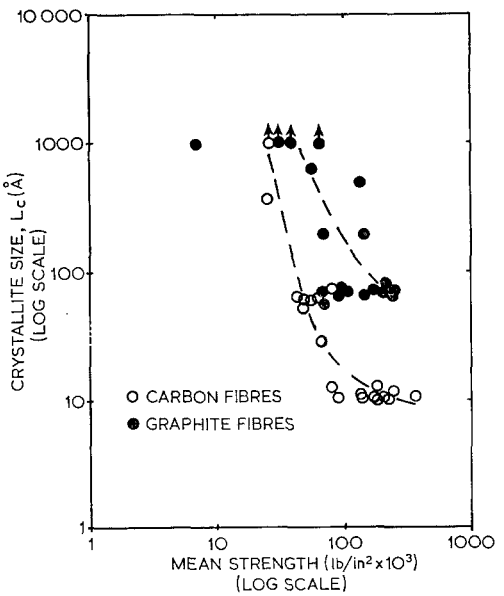

Figure 21 Variation of strength of recrystallised C and G fibres with crystallite size.

The correlation between effective crystallite size and fibre strength is shown in fig. 21. The data reflect both the difficulty of obtaining only partially recrystallised specimens and also the scatter involved in the strength measurements. Because of this scatter no attempt has been made to obtain an empirical relationship.

5. Summary and Conclusions

(i) Techniques have been evolved to study the compatibility of single metal-coated carbon fibres and the results have been shown to be applicable to bulk composites.

(ii) Carbon fibres undergo structural recrystallisation in contact with a nickel or cobalt matrix. This occurs by: (a) detachment of carbon atoms from the fibres and dissolution in the nickel or cobalt; (b) rapid diffusion through the metal; (c) reprecipitation on the fibres or at a new site to grow in a more fully graphitic form.

(iii) Graphitised fibres resist recrystallisation better than carbonised fibres because their more orderly, more stable structure is more resistant to dissolution in the nickel or cobalt matrix.

Acknowledgement

It is a pleasure to acknowledge the assistance of the following colleagues: P. S. Spencer, Mrs L. M. Hallam and R. J. Fowler for fibre coating, heat-treatment and strength testing; Mrs B. Wilkinson and Mrs J. Watkins for the Stereoscan pictures; F. C. Johnson for the C, H, N analyses; D. W. Hocking for assistance with X-ray measurements; J. W. Johnson and C. N. Tyson for many useful discussions and finally B. A. Proctor for his general guidance and encouragement.

References

1. A. E. STANDAGE and R. PRESCOTT, *Nature* **211** (1966) 169.
2. W. WATT, L. N. PHILLIPS, and W. JOHNSON, *Engineer* **221** (1966) 815.
3. W. W. DUNN, R. B. MCLELLAN, and W. A. OATES, *Trans. Met. Soc. AIME* **242** (1968) 2129.
4. J. W. JOHNSON, *J. Applied Polymer Symposia*, 1969 (to be published).
5. P. W. JACKSON and J. R. MARJORAM, *Nature* **218** (1968) 83.
6. W. JOHNSON and W. WATT, *ibid* **215** (1967) 384.
7. F. P. MALLINDER, private communication.
8. P. W. JACKSON, *Metals Engineering Quarterly* **9** (1969) 22.
9. F. JOHNSON, private communication.
10. C. YOKOKAWA, K. HOSOKAWA, and Y. TAKEGAMI, *Carbon* **4** (1966) 459.
11. A. S. SCHWARTZ and J. C. BOKROS, *ibid* **5** (1967) 325.
12. J. C. BOKROS, *J. Nucl. Matls.* **3** (1961) 89.
13. W. D. KINGERY, E. NIKI, and M. D. NARASIMKAN, *J. Amer. Ceram. Soc.* **44** (1961) 29.
14. R. S. WAGNER and W. C. ELLIS, *Trans. Met. Soc. AIME* **233** (1965) 1053.
15. H. M. STRONG, *ibid* **233** (1965) 643.

16. H. M. STRONG and R. E. HANNEMAN, *J. Chem. Phys.* **46** (1967) 3668.
17. J. H. BROPHY, L. A. SHEPARD, and J. WULFF, in "Powder Metallurgy", edited by W. Leszynski (Interscience, New York, 1961) pp. 113-135; J. H. BROPHY, H. W. HAYDEN, and J. WULFF, *Trans. Met. Soc. AIME* **221** (1961) 1225; *Idem, ibid* **224** (1962) 797; H. W. HAYDEN and J. H. BROPHY, *J. Electrochem. Soc.* **110** (1963) 805.
18. I. J. TOTH and N. A. LOCKINGTON, *J. Less-Common Metals* **12** (1967) 353.

Received 16 June and accepted 1 August 1969.

19. J. VACEK, *Planseeberichte fur Pulvermetallurgie* **7** (1959) 6.
20. D. W. PETRASEK and J. W. WEETON, *Trans. Met. Soc. AIME* **230** (1964) 977.
21. C. MATANO, *Mem. Coll. Sci. Kyoto*, **15** (1932) 351 (Quoted in "Metals Reference Book", edited by C. J. Smithells; Butterworths, London, 1962).
22. M. HANSEN, "Constitution of Binary Alloys", 2nd Edition (McGraw Hill, New York, 1958).